

Laser-Cluster Interaction: X-Ray Production by Short Laser Pulses

Cornelia Deiss,* Nina Rohringer, and Joachim Burgdörfer

Institute for Theoretical Physics, Vienna University of Technology, A-1040 Vienna, Austria, EU

Emily Lamour, Christophe Prigent, Jean-Pierre Rozet, and Dominique Vernhet

INSP, Universités Paris 6 et 7, Campus Boucicaut, 75015 Paris, France, EU

(Received 28 June 2005; published 13 January 2006)

We investigate the heating of the quasifree electrons in large rare-gas clusters (N exceeding 10^5 atoms) by short laser pulses at moderate intensities ($I \approx 10^{15}$ W cm $^{-2}$). We identify elastic large-angle backscattering of electrons at ionic cores in the presence of a laser field as an efficient heating mechanism. Its efficiency as well as the effect of collective electron motion, electron-impact ionization, and cluster charging are studied employing a mean-field classical transport simulation. Results for the absolute x-ray yields are in surprisingly good quantitative agreement with recent experimental results.

DOI: [10.1103/PhysRevLett.96.013203](https://doi.org/10.1103/PhysRevLett.96.013203)

PACS numbers: 36.40.Wa, 34.80.Bm, 36.40.Gk, 52.50.Jm

The interaction of short, ultrashort intense laser pulses with clusters has become an important area of laser-matter research bridging the gap between gas-phase and solid-state processes [1]. The observation of characteristic x-ray emission from laser-irradiated clusters [2–5] suggested its potential as an x-ray source through a highly nonlinear conversion of IR radiation that combines the advantages of solid targets (large x-ray yields) and gaseous targets (absence of debris). Characteristic x-ray emission also provides important time-differential information on the laser-induced electronic dynamics on a femtosecond scale. The charge state as well as the vacancy distribution of the cluster ions at the instant of emission can be extracted from high-resolution x-ray spectra. Moreover, as the vacancy production in deeply bound shells (e.g., K shell in argon) proceeds via impact ionization by energetic electrons, characteristic x-rays provide an “*in situ*” thermometer of the temperature of the heated electron gas in the cluster. Recent experiments [3–5] found an unexpectedly low laser intensity threshold for the production of x-ray radiation. When irradiating large argon clusters with $N > 10^5$ atoms with laser pulses with a short pulse duration of $\tau = 60$ fs at FWHM and wavelength $\lambda = 800$ nm, the intensity threshold for the production of characteristic K -x-rays lies at $I_{\text{th}} \approx 2.2 \times 10^{15}$ W cm $^{-2}$. By comparison, the ponderomotive energy, $U_p = F^2/(4\omega^2)$, of a free electron in a laser field of this intensity is $U_p \approx 130$ eV, more than an order of magnitude below the binding energy $E_K \approx 3.2$ keV of the K -shell electrons. This observation raises puzzling questions as to the heating mechanism for electrons in large clusters at such moderate intensities of very short pulses with ~ 40 optical cycles.

Several theoretical models for intense laser-cluster interaction have been proposed [1,6–11], none of which appears to provide a satisfactory explanation for such rapid acceleration of electrons. A theoretical description represents a considerable challenge in view of the many-body nature of this process. Molecular dynamic simulations [7–9] are limited to about 1000 atoms, and results obtained for

small clusters are difficult to scale to larger sizes. The recently proposed microscopic particle in cell method (MPIC) [10] reaches clusters of $\sim 10^4$ atoms. Larger clusters with $N > 10^5$ particles appear still not in reach, and quantitative predictions for x-ray emission and inner-shell processes have not yet been attempted. In this Letter, we propose a heating mechanism of electrons in large clusters that is operational within a few optical cycles and at moderate laser intensities. It is based on the observation that *elastic* large-angle scattering of electrons at cluster atoms (ions) in the simultaneous presence of a laser field provides an efficient route to electron acceleration. Elastic backscattering at the core potential of the ions can flip the velocity vector of an electron, such that a subensemble of electrons has non-negligible probability to remain synchronized with the alternating laser field vector during the subsequent half cycle (Fig. 1). Consequently, such electrons will rapidly accumulate rather than lose momentum during subsequent half cycles. Within a few optical cycles, electrons can thus be accelerated to high kinetic energies well beyond the maximum quiver energy $E_p = 2U_p$. This heating mechanism by repeated backscattering resembles the Fermi shuttle acceleration [12,13] and is also related to the lucky-electron model proposed for IR photoemission from metallic surfaces [14]. A realistic estimate for the efficiency of this heating mechanism hinges on a proper description of the differential elastic scattering cross sections for electrons, $d\sigma_e/d\theta$, into backward angles $\theta \gtrsim 90^\circ$, which are determined by the non-Coulombic short-ranged potentials of the ionic cores. $d\sigma_e/d\theta$ was calculated for electron scattering at argon ions for all charge states over a wide range of energies by partial wave analysis of parametrized Hartree-Fock potentials [15,16]. $d\sigma_e/d\theta$ is typically dominated by few low-order partial waves giving rise to generalized Ramsauer-Townsend minima [17] and diffraction oscillations [18] (Fig. 2). We assumed for simplicity the electronic ground state occupation for each charge state q . Extensions to core-excited configurations would be straight forward.

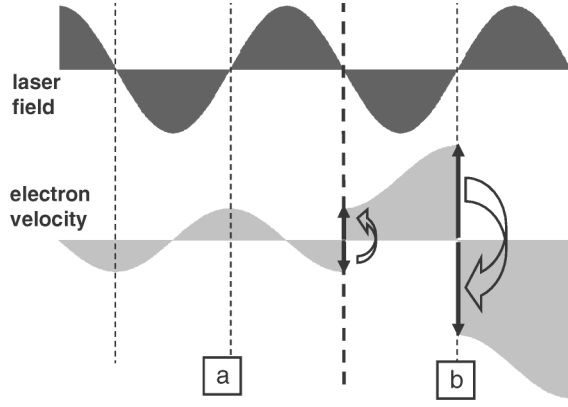


FIG. 1. Time evolution of the velocity of an electron in a laser field, schematically. A free electron does not experience effective velocity gain beyond the quiver velocity (a). If the velocity is flipped, an electron can rapidly absorb kinetic energy from the laser field (b). This process is operational only for a subensemble of electrons (see text).

For the interstitial region a muffin-tin potential is employed in order to account for solid-state effects [16]. The potential shape in this region, however, has no influence on the cross section at backward angles. The latter exceeds the pure Coulomb case by several orders of magnitude for all charge states and over a wide range of electron energies (\approx keV). The frequent usage in simulations of unrealistic (softened) Coulomb potentials [7,9,10], which grossly underestimates backscattering, is quite likely one reason why this route of electron acceleration has not yet been accounted for. Moreover, this process becomes more important for large clusters, as the mean-free path for elastic scattering becomes comparable to the cluster size. The important role of realistic core potentials has recently also been identified in the quantum analogue

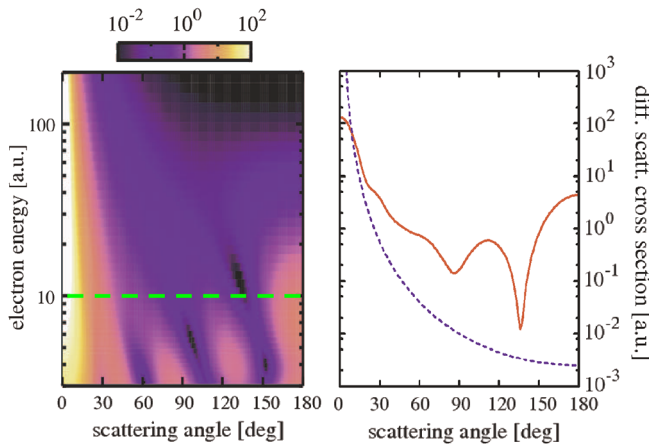


FIG. 2 (color online). Left: Differential cross-section distribution $d\sigma_e(\theta, E)/d\Omega$ in a.u. for elastic electron scattering at Ar^{2+} ions. Right: $d\sigma_e(\theta)/d\Omega$ for an electron with fixed kinetic energy $E = 10$ a.u. (solid line). For comparison, the Rutherford cross section $(\frac{q}{4E})^2 \frac{1}{\sin^4(\theta/2)}$ is also displayed (dashed line).

of this process, inverse bremsstrahlung ($U_P \ll \hbar\omega$), for clusters in a vacuum ultraviolet laser field [19].

A full *ab initio* simulation for large clusters ($N \geq 10^5$ particles) appears still impractical. In the following, we present a simplified theoretical description of the electronic ensemble that allows one to tackle its short-time dynamics ($\tau \sim 60$ fs). It employs a generalization of classical transport theory (CTT) [20] for open systems, in which the electronic dynamics is represented by a classical phase-space distribution $f(\mathbf{r}, \dot{\mathbf{r}}, t)$ whose evolution is determined by test-particle discretization, i.e., by solving the corresponding Langevin equation for representative trajectories (atomic units are used unless otherwise stated):

$$\ddot{\mathbf{r}}_i = -\mathbf{F}_L(t) - \nabla V(\mathbf{r}_i, t) - \mathbf{F}_{\text{mean}}(\mathbf{r}_i, t) + \mathbf{F}_{\text{stoc}}(\mathbf{r}_i, \dot{\mathbf{r}}_i, t). \quad (1)$$

The ensemble consists of N_e quasifree electrons, liberated inside the cluster after ionization of the cluster atoms, represented by $i = 1, \dots, N_{\text{test}}(t) = \alpha N_e(t)$ particles, where the representation fraction α is limited by computational feasibility. Equation (1) describes a dynamical system open to both particle number variation, $N_{\text{test}}(t)$, due to successive ionization events, and energy exchange with the many-particle reservoir (atoms, ions, and electrons) as well as with the laser field taken to be linearly polarized with a temporal envelope,

$$\mathbf{F}_L(t) = F_0 \hat{\mathbf{z}} \sin(\omega t) \sin^2\left(\frac{\pi t}{2\tau}\right). \quad (2)$$

Equation (1) provides a computational starting point for treating many-body collisional correlation effects through stochastic forces \mathbf{F}_{stoc} , which can be determined either from independent *ab initio* quantum calculations or experimental data [20]. Forces resulting from static conservative potentials V inside the cluster [7] can be included as well. Because of the coherent motion and high ionization density, the present extension of the CTT (1) goes beyond the independent-particle description by including dynamic electron-electron and electron-ion interactions on a time-dependent mean-field level. Accordingly, \mathbf{F}_{mean} depends on the entire ensemble of test-particle coordinates $\{\mathbf{r}_i(t)\}$.

Effects of fluctuations on the electronic dynamics can be taken into account through stochastic forces which are determined from Poissonian random processes. For example, electron-ion scattering, electron-impact ionization, and core-hole excitation are determined by the probability per unit path length for scattering

$$\lambda_{\text{scatt}}^{-1} = \frac{dP_{\text{scatt}}}{dx} = \sigma_{\text{scatt}}(q, E)\rho(t), \quad (3)$$

controlled by the energy (E) and q dependent integral cross section for this process, $\sigma_{\text{scatt}}(q, E)$, and the instantaneous ionic target density $\rho(t)$ of a given charge state. Each stochastic scattering process results in “jumps” (classical trajectory jumps and jumps in occupation) at discrete times. A jump in momentum, $\Delta\dot{\mathbf{r}}$, signifies elastic scatter-

ing determined by the differential cross section, $d\sigma_e(q, E, \theta)/d\theta$, a simultaneous jump in test-particle number, ΔN_{test} , represents ionizing collisions, and a simultaneous jump in the number of inner-shell vacancies, ΔN_K , results from core-exciting collisions. The key point is that the necessary input data, $\sigma_{\text{scatt}}(q, E)$, can be determined and tabulated independently from the simulation. In the present simulation, the electron-impact ionization cross sections are determined from a modified Lotz formula [4,21]: $\sigma_i(q, E) = A_q^* \ln(E/W_q^*)/(EW_q^*)$ (for $E \geq W_q^*$), where the empirical parameters A_q^* and W_q^* were obtained by a fit to experimental ion-atom collision data [4,22].

For the mean field, we perform a multipole expansion keeping only the monopole and dipole terms. The monopole term is given by $\mathbf{F}_{\text{mean}}^{(0)}(\vec{r}, t) = \langle Q(r, t) \rangle \mathbf{r}/r^3$, where $\langle Q(r, t) \rangle$ is the instantaneous charge of the sphere of radius r resulting from the displacement of the ensemble of test particles relative to the ionic background. Analogously, the dipole field inside the cluster [$r < R(t)$] is $\mathbf{F}_{\text{mean}}^{(1)}(t) = -\mathbf{p}(t)/R(t)^3$, while outside it is that of a central dipole. The dipole moment, \mathbf{p} is determined by $\mathbf{p}(t) \approx -\frac{1}{\alpha} \sum_i \mathbf{r}_i$, where the sum extends over the subset of test particles with $r_i < R(t)$.

As the ionic and electronic dynamics proceed on different time scales, the onset of cluster expansion can be taken into account through the parametric variation of the radius $R(t)$ of the uniform spherical charge background representing the ions of mass M in their time-dependent mean charge state $\langle q(t) \rangle$:

$$M \frac{d^2 R(t)}{dt^2} = \frac{\langle q(t) \rangle \langle Q(R, t) \rangle}{R^2(t)}. \quad (4)$$

We solve Eq. (1) for a cluster with $N = 2.8 \times 10^5$ argon atoms with initial atomic number density $\rho(t=0) = 2.66 \times 10^{22} \text{ cm}^{-3}$ and initial radius $R(0) = 258 \text{ a.u.}$ irradiated by a short infrared laser pulse. As the laser field reaches for the first time the threshold field for over-barrier ionization $F_L(t_1) \approx 0.08$, the first $N_{\text{test}}(t_1)$ test particles with zero velocity randomly distributed over the cluster provide initial conditions for the propagation of Eq. (1). In the present case $N_{\text{test}} = 0.1N_e$ (or $\alpha = 0.1$). Contributions from tunneling ionization can be included but are in the present case negligible. The test-particle number subsequently increases by further ionization events [Fig. 3(a)]. While a free atom in the laser field could reach only a maximum charge state of $q = 4$ by over-barrier ionization, electron-impact ionization rapidly increases the mean charge state of the atoms in the cluster to ~ 7 . This result most likely still underestimates the ionization efficiency, as nonradiative core-hole relaxation and enhanced ionization by suppression of the work function by ion proximity are not yet included. The Coulomb expansion of the cluster sets in slowly due to the large inertia of the ions. Even after the laser pulse is switched off ($t \approx 2\tau$), the cluster has expanded by less than a factor of 2. Our simulation shows that the charge resulting from electrons leaving the cluster

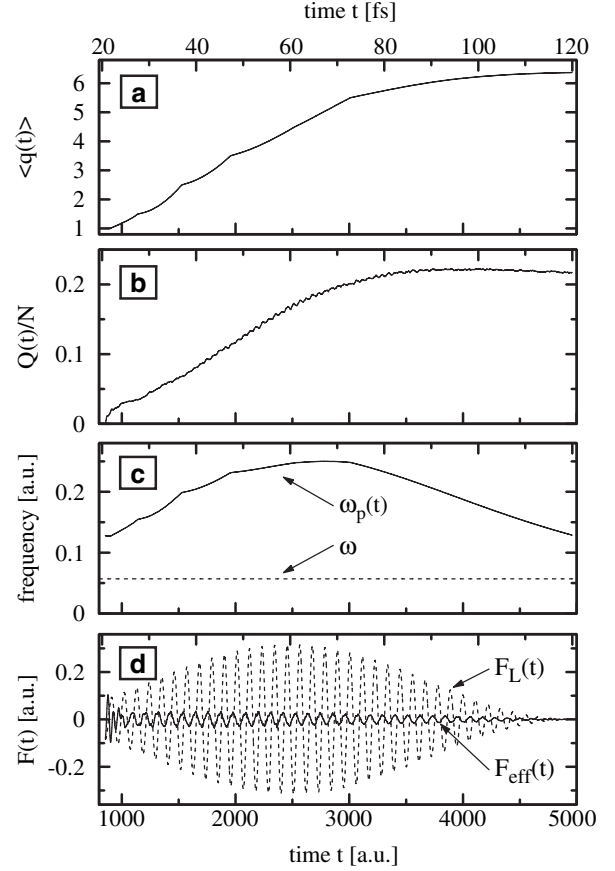


FIG. 3. Dynamics of an argon cluster with $N = 2.8 \times 10^5$ atoms, irradiated by a laser pulse with wavelength $\lambda = 800 \text{ nm}$, duration $\tau = 60 \text{ fs}$, and peak intensity $I = 3.5 \times 10^{15} \text{ W cm}^{-2}$. All quantities are shown as a function of time. (a) Mean ionic charge state $\langle q(t) \rangle$, (b) cluster charge per atom $Q(t)/N$, (c) comparison between plasma frequency $\omega_p(t)$ (solid line) and laser frequency ω (dashed line), and (d) effective field $F_{\text{eff}} = F_L + F_{\text{mean}}^{(1)}$ inside the cluster (solid line) and laser field F_L (dashed line).

[Fig. 3(b)] is concentrated on the surface of the cluster, the ions in the inside of the cluster being well shielded by the quasifree electrons, in agreement with the MPIC simulation [10]. After the production of Ar^{1+} the electronic plasma frequency is given by $\omega_p^2 = N_{\text{test}}(t_1)/(\alpha R(t_1)^3) = \rho(t_1)4\pi/3 \approx 5\omega^2$. As electron-impact ionization produces more quasifree electrons, ω_p grows rapidly before diminishing again as the cluster expansion sets in [Fig. 3(c)]. The simulated effective field inside the cluster [Fig. 3(d)] $F_{\text{eff}} = F_L + F_{\text{mean}}^{(1)}$ can also be estimated following Ref. [6]:

$$\begin{aligned} \vec{F}_{\text{eff}}(t) = \text{Re} \left\{ \int_{\omega-\Delta\omega}^{\omega+\Delta\omega} \vec{F}_L(\omega') \right. \\ \left. \times \left(1 - \frac{\omega_p^2}{\omega_p^2 - \omega'^2 - i\omega'\gamma} \right) e^{i\omega't} d\omega' \right\}, \quad (5) \end{aligned}$$

where $\Delta\omega$ is the Fourier width caused by the temporal profile of the pulse (2) and γ stands for the damping due to

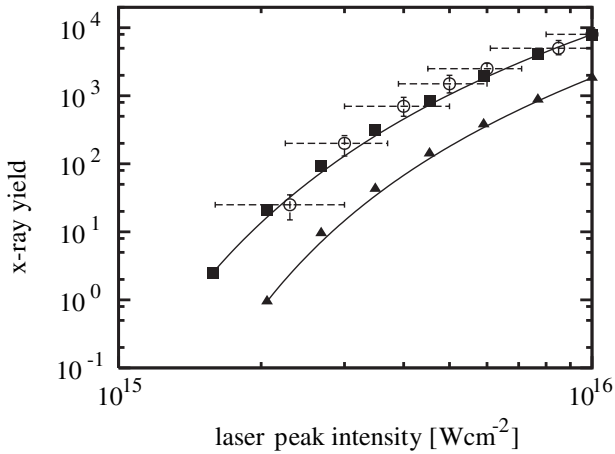


FIG. 4. Absolute x-ray yield as a function of the laser peak intensity. Experimental results [4] (\circ), simulation results obtained with a Coulomb potential (\blacktriangle), and with the realistic ionic potential (see text) (\blacksquare).

scattering events. F_{eff} (or \bar{F}_{eff}) is significantly reduced compared to the bare laser field [Fig. 3(d)] due to the combined effect of collective electron motion and electron-impact ionization. A significant resonant enhancement [6,9] is absent. Furthermore, the evaluation of $L = \int \mathbf{J} \mathbf{F}_{\text{eff}} dt$ (see Ref. [10]) shows that dephasing of the electronic current \mathbf{J} with respect to the driving field due to the macroscopic electric field inside the cluster, leads in our case only to a negligible net energy absorption of $L \sim 0.25$ a.u..

The efficiency of heating by elastic electron-ion scattering is directly reflected in the simulated absolute x-ray yield (Fig. 4). The latter is determined by the number of K -shell vacancies created, corrected for the mean fluorescence yield η taken to be $\eta \approx 0.12$ [23] for argon with partially filled L shell but empty M shell. It should be emphasized that the simulation contains no freely adjustable parameter. To compare the simulation results to the experiments, an ensemble average over the Gaussian spatial intensity profile [4] of the laser beam is performed. To quantify the significance of the acceleration by repeated elastic backscattering, we performed an otherwise identical simulation with differential scattering cross sections extracted from a Coulomb potential. In this case for $I \geq 2 \times 10^{15} \text{ W cm}^{-2}$ a small fraction of quasifree electrons gains sufficient energy to produce K -shell vacancies. Their mean kinetic energy can be estimated from the potential energy of the charged-up cluster with charge $Q(t)$ (i.e., the monopole term of the mean effective field). However, including the realistic scattering potential drastically increases the x-ray yield by a factor 4 to 7. We then find surprisingly close agreement with the experimental results (Fig. 4).

In summary, we have analyzed the heating of the quasifree electrons in large rare-gas clusters ($N \sim 10^5$ atoms) at moderate laser intensities ($I = 10^{15} - 10^{16} \text{ W cm}^{-2}$). We

have identified a highly efficient electron heating mechanism operative at short times within a few optical cycles in terms of elastic large-angle scattering using realistic atomic potentials. Other processes such as acceleration of ionized electrons from nearby nonclustered atoms in the Coulomb field of the cluster [24] or heating in a plasma-resonant field are found to be less effective. In particular, the polarization of the cluster leads to a reduction rather than an enhancement of the effective field. While the surprisingly good quantitative agreement on an absolute scale with experimental data may be, in part, fortuitous, the importance of this route to fast electron acceleration appears unambiguously established.

This work is supported by FWF SFB-16 (Austria).

*Electronic address: cornelia@concord.itp.tuwien.ac.at

- [1] V.P. Krainov and M.B. Smirnov, Phys. Rep. **370**, 237 (2002).
- [2] L. Adoui *et al.*, Nucl. Instrum. Methods Phys. Res., Sect. B **205**, 341 (2003).
- [3] E. Lamour *et al.*, Nucl. Instrum. Methods Phys. Res., Sect. B **235**, 408 (2005).
- [4] Christophe Prigent, Ph.D. thesis, Université Pierre et Marie Curie, Paris VI, 2004.
- [5] C. Prigent *et al.* (to be published).
- [6] T. Ditmire *et al.*, Phys. Rev. A **53**, 3379 (1996).
- [7] I. Last and J. Jortner, J. Phys. Chem. A **102**, 9655 (1998); Phys. Rev. A **60**, 2215 (1999).
- [8] C. Rose-Petrucci *et al.*, Phys. Rev. A **55**, 1182 (1997).
- [9] U. Saalmann and J.M. Rost, Phys. Rev. Lett. **91**, 223401 (2003).
- [10] C. Jungreuthmayer *et al.*, Phys. Rev. Lett. **92**, 133401 (2004).
- [11] M.B. Smirnov and W. Becker, Phys. Rev. A **69**, 013201 (2004).
- [12] E. Fermi, Phys. Rev. **75**, 1169 (1949).
- [13] J. Burgdörfer, J. Wang, and R.H. Ritchie, Phys. Scr. **44**, 391 (1991).
- [14] F. Pisani *et al.*, Phys. Rev. Lett. **87**, 187403 (2001).
- [15] P.P. Szydlík and A.E.S. Green, Phys. Rev. A **9**, 1885 (1974).
- [16] F. Salvat and R. Mayol, Comput. Phys. Commun. **74**, 358 (1993).
- [17] N. Mott and H. Massey, *Theory of Atomic Collisions* (Oxford University Press, New York, 1965).
- [18] J. Burgdörfer *et al.*, Phys. Rev. A **51**, 1248 (1995).
- [19] R. Santra and C.H. Greene, Phys. Rev. Lett. **91**, 233401 (2003).
- [20] J. Burgdörfer and J. Gibbons, Phys. Rev. A **42**, 1206 (1990); J. Burgdörfer, in *The Physics of Electronic and Atomic Collisions*, edited by A. Dalgarno *et al.*, AIP Conf. Proc. No. 205 (AIP, New York, 1990), p. 476.
- [21] W. Lotz, Z. Phys. **216**, 241 (1968).
- [22] H. Zhang *et al.*, J. Phys. B **35**, 3829 (2002).
- [23] C.P. Bhalla, Phys. Rev. A **8**, 2877 (1973).
- [24] P. Mulser, M. Kanopathipillai, and D.H.H. Hoffmann, Phys. Rev. Lett. **95**, 103401 (2005).